

Fibrinogen is a ligand for the *S. aureus* MSCRAMM Bbp (Bone sialoprotein-binding protein)
Vanessa Vazquez^{‡,¶}, Xiaowen Liang[‡], Jenny K. Horndahl[‡], Vannakambadi K. Ganesh[‡], Emanuel Smeds[‡],
Timothy J. Foster[§], Magnus Hook^{‡**}

[‡]Center for Infectious and Inflammatory Diseases, Institute of Biosciences and Technology, Texas A&M University System Health Science Center, Houston, TX 77030. [¶]Graduate School of Biomedical Sciences, University of Texas Health Science Center, Houston, TX 77030. [§]Moyne Institute of Preventive Medicine, Department of Microbiology, Trinity College, Dublin, Ireland.

** To whom correspondence should be addressed: Center for Infectious and Inflammatory Diseases, Texas A&M University System Health Science Center, Institute of Biosciences and Technology, 2121 West Holcombe Blvd., Suite 603, Houston, TX 77030, Tel.: 713-677-7551; Fax: 713-677-7576; E-mail: mhook@ibt.tamhsc.edu.

Running Title: Fibrinogen is a ligand for the *S. aureus* MSCRAMM Bbp

ABSTRACT

MSCRAMMs (microbial surface components recognizing adhesive matrix molecules) are bacterial surface proteins mediating adherence of the microbes to components of the extracellular matrix of the host. On Staphylococci the MSCRAMMs often have multiple ligands. Consequently we hypothesized that the *S. aureus* MSCRAMM Bbp (bone sialoprotein-binding protein) might recognize host molecules other than the identified bone protein. A ligand screen revealed that Bbp binds human fibrinogen (Fg) but not Fg from other mammals. We have characterized the interaction between Bbp and Fg. The binding site of Bbp was mapped to residues 561-575 in the Fg A α chain using recombinant Fg chains and truncation mutants in Far Western blots and solid phase binding assays. Surface plasmon resonance was used to determine the affinity of Bbp for Fg. The interaction of Bbp with Fg peptides corresponding to the mapped residues was further characterized using isothermal titration calorimetry. In addition, Bbp expressed on the surface of bacteria mediated adherence to immobilized Fg A α . Also, Bbp interferes with thrombin-induced Fg coagulation. Together these data demonstrate that human Fg is a ligand for Bbp and that Bbp can manipulate the biology of the Fg ligand in the host.

INTRODUCTION

Staphylococcus aureus uses secreted and cell-surface associated virulence factors to cause disease ranging from mild skin infections like folliculitis and impetigo to life-threatening illnesses like sepsis, and pneumonia (1).

MSCRAMMs (Microbial surface components recognizing adhesive matrix molecules) are surface proteins used by bacteria to interact with host molecules such as collagen, fibronectin, and fibrinogen (Fg). The Sdr proteins are a subset of putative staphylococcal MSCRAMMs, covalently anchored to the cell-wall and characterized by a segment composed of repeated serine-aspartate (SD) dipeptides. The Sdr proteins have similar structural organization where the N-terminal ligand-binding A region can be further divided into three sub-domains (N1, N2, and N3), where N2 and N3 adopt IgG-like folds. The A-region is often followed by a B region that consists of repeated β -sandwich domains. The carboxy-terminal section of the proteins contains the serine-aspartate repeats followed by motifs required for cell-wall anchoring (2).

A dynamic ligand binding mechanism called the “dock, lock and latch” was revealed by biochemical and structural studies of the fibrinogen binding *S. epidermidis* MSCRAMM SdrG (3). SdrG binds to a linear sequence in the N-terminus of the B β chain of human Fg. The SdrG binding sequence includes the thrombin cleavage site, and the MSCRAMM inhibits thrombin-catalyzed release of fibrinopeptide B and fibrin formation (3, 4). Binding is initiated by the “docking” of the ligand peptide into the trench formed between the N2 and N3 IgG-domains.

Next, the ligand is “locked” in place by interactions with residues at the extension of the C-terminus of N3 that are redirected to cover the bound ligand peptide. Following the “lock” event the “latch” region in the N3 extension stabilizes the ligand/MSCRAMM complex by inserting into the N2 domain through a β -strand complementation (3, 5). Because the Sdr proteins are similar in domain organization and folding, the “dock, lock, and latch” mechanism has been proposed as a general mechanism of ligand binding for this sub-family of MSCRAMMs.

Fibrinogen is a large dimeric protein composed of three polypeptides, $\text{A}\alpha$, $\text{B}\beta$, and γ , with key roles in blood coagulation, thrombosis, and host defense (6-8). Known Fg-binding MSCRAMMs on *S. aureus* include the clumping factors (ClfA and ClfB) and the fibronectin-binding proteins (FnbpA and FnbpB) (9), (10), (11), (12). ClfB binds to a site in the central part of the $\text{A}\alpha$ chain C-terminus while ClfA and the FnBPs bind to the extreme C-terminus of the Fg γ chain (13), (14), (11). Each of these Fg-binding MSCRAMMs interacts with additional ligands. ClfA binds to complement factor I (15), and ClfB binds to cytokeratin 10 (16). FnbpA binds to elastin and both FnbpA and FnbpB bind to fibrinogen (11),

We hypothesized that Bbp might also recognize multiple host proteins. A ligand screen revealed that Bbp_{N2N3} recognizes human Fg and the initial characterization of this interaction is reported here.

EXPERIMENTAL PROCEDURES

Media and growth conditions—*Escherichia coli* strains were cultured at 37°C with shaking in Luria broth (Sigma) supplemented with ampicillin (100 $\mu\text{g}/\text{ml}$). *Lactococcus lactis* was cultured in M17 (Oxoid) supplemented with glucose (0.5%) and erythromycin (5 $\mu\text{g}/\text{ml}$) at 30°C overnight. *Staphylococcus aureus* MRSA 252 was cultured in BHIB (Remel) at 37°C with shaking. *S. aureus* Newman derivatives were cultured in BHIB supplemented with erythromycin (5 $\mu\text{g}/\text{ml}$), tetracycline (2 $\mu\text{g}/\text{ml}$), and/or chloramphenicol (10 $\mu\text{g}/\text{ml}$) as needed to exponential phase.

Recombinant proteins – A recombinant Bbp construct corresponding to the (N2N3 domains) amino acids 270-599 of previously published sequences was engineered (17). The amplification primer sequences are listed in Table 1. All oligonucleotides used for this study were purchased from IDT. *E. coli* expressing full-length recombinant His-tagged Fg chains $\text{A}\alpha$, $\text{B}\beta$, and γ have been previously described (18-20). A plasmid encoding the Fg $\text{A}\alpha$ sequence was used as template to amplify the DNA encoding truncated $\text{A}\alpha$ protein corresponding to residues 1-575 and 1-560. Selected plasmids were digested, the inserts ligated to pQE30, and transformed into XL-1 Blue cells, followed by sequence verification of plasmids pQE30-Bbp_{N2N3}, pQE30-A α 1-575 and pQE30-A α 1-560. Recombinant protein expression was induced with IPTG (Gold Biotechnology), and expressed protein was purified by Ni²⁺ affinity chromatography on a HiTrap Chelating column (GE Healthcare) followed by anion exchange-chromatography using a Q HP Sepharose (GE Healthcare), as previously described (4). The His-tagged recombinant Fg chains, $\text{A}\alpha$, $\text{A}\alpha$ 1-560, $\text{A}\alpha$ 1-575, $\text{B}\beta$, and γ were recovered from inclusion bodies and purification was performed in the presence of 8M Urea (Sigma). To assess protein purity pooled fractions were separated on 10% SDS-PAGE and stained with Coomassie blue or electrotransferred to nitrocellulose for Western blotting with anti-His monoclonal (GE Healthcare), followed by anti-mouse-AP (Bio-Rad). The mass of Bbp_{N2N3} was determined to be 37,491.4 Daltons (not shown) by mass spectrometry, which is similar to the predicted mass of 37,837.6 Daltons.

Rabbit-anti-Bbp_{N2N3} antibodies – Rabbit polyclonal antiserum to Bbp_{N2N3} was generated at Rockland Immunochemicals under the Fast Production Protocol. IgG was purified using protein A-sepharose (ThermoFisher) affinity chromatography. Next, the IgG was cleared for crossreactive binding to other Sdr proteins before positive affinity purification on Bbp_{N2N3} coupled to EZlink beads (ThermoFisher). This preparation, followed by goat-anti-rabbit HRP, was used to detect Bbp_{N2N3} binding in solid-phase assays.

Homology modeling– The predicted ligand binding subdomains of Bbp_{N2N3} were modeled based on the previously determined crystal

structure of SdrG (3). The SdrG_{N2N3} and Bbp_{N2N3} share approximately 50% sequence identity. The homology modeling was performed using “Homology” module in the InsightII software (Accelrys Inc.). The ribbon figure was made with RIBBONS software (21).

Solid-phase binding assays- To conduct a Bbp_{N2N3} ligand screen with extracellular matrix and plasma proteins, 1 µg of human fibrinogen depleted of plasminogen and von Willebrand Factor (Enzyme Research) human fibronectin (Chemicon), BSA, collagen type I from rat tail tendons (Cultrex R&D), bovine nasal septum type II collagen (Sigma), recombinant human collagen type III (Fibrogen), fibroblast and epithelial cell co-culture collagen type IV (Sigma), and bovine neck ligament elastin (Sigma), or 10 µg of murine sarcoma basement membrane laminin (Sigma) were coated on microtiter wells overnight. The wells were washed, blocked and incubated with 100 µl of Bbp_{N2N3} (0.1-10 µM) and developed with anti-His tag antibodies.

To detect binding of immobilized Bbp to soluble Fg, microtiter wells were coated with increasing amounts of Bbp_{N2N3} (0.25-2.5 µg). The wells were washed, blocked, probed with 100 µl soluble Fg (1 µM) and developed with goat anti-human fibrinogen (Sigma) followed by donkey anti-goat-HRP (Applied Biological Materials).

To determine binding of MSCRAMMs to Fg, microtiter wells were coated with 1 µg of human, mouse (Enzyme Research), cat, dog, cow, sheep, and pig (Sigma) fibrinogen, or recombinant human Fg polypeptides. The wells were subsequently washed, blocked, and probed with 100 µl Bbp_{N2N3} or ClfA_{N2N3} at the indicated concentrations followed by protein-specific rabbit antibodies and goat anti-rabbit HRP (Bio-Rad).

In peptide inhibition experiments 150 nM Bbp_{N2N3} was incubated with increasing concentrations (0.1 to 30 µM) of Fg Aα peptides synthesized by Biomatik (Table 3) for 30 minutes before 100 µl of the mixture was transferred to Fg-coated wells. MSCRAMM binding was detected as described above.

All proteins were coated at 4°C in bicarbonate buffer pH 8.3. All wells were washed with Tris buffered saline containing 0.1% Tween-20, blocked with Superblock (ThermoFisher), developed with SigmaFast OPD, and the

absorbance at 450 nm was measured using a Thermo Max plate reader and plotted with GraphPad Prism 4.

Surface Plasmon Resonance (SPR) – SPR analysis was performed at 25°C on a BIAcore 3000 system using a CM5 chip (GE Healthcare). The ligand surface was prepared via amine coupling. Fg (12 µl of 10 µg/ml in sodium acetate, pH 5.5) was injected over an activated flow cell at 5 µl/min for 3 minutes using HEPES-buffered saline containing 0.005% Tween-20 as the running buffer. Approximately 1600 response units (RU) of human Fg were immobilized. A second uncoupled flow cell was activated and deactivated to serve as a reference cell. Increasing concentrations of Bbp_{N2N3} (40 nM-2.56 µM in TBS-0.005% Tween 20) were injected at 30 µl/min over ligand and reference surfaces. After subtraction of reference cell from the experimental cell sensorgrams, the baseline-corrected SPR response curves were globally fitted to the 1:1 (Langmuir) binding model using BIAevaluation software. Association and dissociation rate constants (k_a , k_d) were obtained from the fitting and a dissociation constant (K_D) was calculated ($K_D = k_d / k_a$). Responses at equilibrium of the SPR curves were fitted to a one-site binding isotherm (GraphPad Prism 4) to obtain the equilibrium K_D and binding maximum (B_{max}).

SDS-PAGE and Far Western blot of Fg- Human and recombinant Fg proteins were separated on 10% SDS-PAGE using Laemmli sample buffer containing 10 mM dithiothreitol followed by Coomassie blue staining or electrotransfer to nitrocellulose membrane. Membranes were blocked with TBST containing 1% BSA followed by probing with Bbp_{N2N3} (15 µg/ml), ClfA_{N2N3} (15 µg/ml), or SdrG_{N2N3} (5 µg/ml). The bound proteins were detected with anti-His monoclonal antibody followed by anti-mouse-AP or rabbit anti-Bbp_{N2N3}. Membranes were developed using NBT/BCIP (ThermoFisher).

Lactococcus lactis-Bbp- The entire *bbp* coding region from strain *S. aureus* B504 (kindly donated by Ed Feil) was ligated into the pKS80 plasmid for constitutive expression (22). The plasmid pKS80-Bbp was transformed into *Lactococcus lactis* MG1363 and plated on GM17 supplemented with erythromycin.

S. aureus Newman expressing -Bbp – The *bbp* promoter, coding, and terminator DNA

segment from *S. aureus* MRSA252 (kindly provided by NARSA) was subcloned into TOPO-Zero Blunt. Following digestion with BamHI and XbaI, the insert was ligated to the shuttle vector pCU1, and the plasmid pCU1-Bbp was transformed into *E. coli* XL-10 Gold cells (Stratagene). The plasmid was purified and transformed into electrocompetent *S. aureus* RN4220 and plated on BHIB with chloramphenicol. Subsequently, pCU1-Bbp was electroporated into electrocompetent Newman DU6023 *clfA5 isdA clfB::Em^r ΔsdrCDE::Tc^r* cells (23).

Bacterial adherence assays: *L. lactis*-pKS80-Bbp, *L. lactis*-pKS80, *S. aureus* Newman DU6023-pCU1-Bbp, and Newman DU6023-pCU1 cells were washed, and resuspended to OD₆₀₀ of 1.0 or 2.0 for *L. lactis* and *S. aureus*, respectively, in PBS supplemented with 0.5 mM magnesium chloride and 0.1 mM calcium chloride. Microtiter wells were coated with Fg Aα1-560 or Fg Aα1-575, washed, and blocked with PBS-1%BSA. Wells were incubated with 0.1 ml of bacterial suspension for 1.5 hours at 30°C for *L. lactis* or 37°C for *S. aureus* strains. Attached bacteria were detected by crystal violet staining as previously described (23).

Isothermal titration calorimetry (ITC)– The interaction between Bbp_{N2N3} protein and soluble Fg Aα peptides (Table 3) was analyzed using a VP-ITC microcalorimeter (MicroCal) at 30°C in TBS. The cell contained 15 μM Bbp_{N2N3}, and the syringe contained 225 μM. Samples were degassed for 5 minutes and titration was performed with a stirring speed of 300 rpm. The initial injection was 5 μl followed by 29 injections of 10 μl at 0.5 μl/second. Data were fitted to a single binding site model and analyzed using Origin version 5 (MicroCal) software.

Multiple sequence alignment – Sequences corresponding to the mapped Fg Aα residues from different species were aligned using Clustal W version 2 (24). The sequence gi numbers are as follows: 1304047 – Canine; 3789958 – Feline; 296478815 – Bovine; 1304179 – Porcine; 33563252 – Murine; and 11761629 – human.

Fibrin inhibition assay– Thrombin-catalyzed fibrinogen clotting was studied as previously described (4). Briefly, 150 μl of a 3.0 μM Fg solution was incubated with 10 μl of increasing concentrations (0.3-10 μM) of Bbp_{N2N3},

SdrG_{N2N3}, or BSA and 50 μl of thrombin (1.0 NIH unit/ml) in microtiter wells. Clot formation was monitored by measuring the increase in A₄₀₅ and plotted using GraphPad 4.

RESULTS

Bbp_{N2N3} binds to human fibrinogen – The known ligand binding sites of other MSCRAMMs of the Sdr family have been mapped to the N2N3 domains of the N-terminal A-region of the proteins. We first defined the putative N2N3 domains of Bbp to residues 270-599 (Fig. 1A, 1B) by comparing the sequence of Bbp to that of SdrG and ClfA for which we have previously determined the crystal structures (4), (25), (26). This segment was expressed as a recombinant His-tagged fusion protein and purified using affinity and ion-exchange chromatography (Fig. 1C). To explore the ligand binding of Bbp we conducted an initial screen where increasing concentrations (0.01 to 10.0 μM) of recombinant His-tagged Bbp_{N2N3} were incubated in microtiter wells coated with a selection of extracellular matrix and plasma proteins (Fig. 2A). In this assay, Bbp_{N2N3} bound to Fg in a concentration-dependent, saturable manner but failed to bind to elastin, collagen types I – IV, laminin, fibronectin, and albumin. We also found that soluble Fg bound to increasing amounts of Bbp_{N2N3} coated on microtiter wells (Fig. 2B). Thus the solid phase assays indicate a specific interaction between Bbp_{N2N3} and Fg regardless of which was immobilized.

We next determined the species specificity of the Fg recognized by Bbp. Human, feline, canine, bovine, ovine, murine or porcine Fg were used to coat microtiter wells and the binding of Bbp_{N2N3} to the Fg coated surfaces was measured. Our results indicate that Bbp_{N2N3} only binds to Fg isolated from human plasma (Fig. 2C). These results suggest that Bbp recognizes a specific motif present in human Fg but not found in other Fgs. This restricted specificity is in contrast to that of ClfA, which binds to all of the Fgs tested with the exception of ovine Fg (Fig. 2C).

The dissociation constant of the Bbp_{N2N3}/Fg complex was determined using SPR. Binding of increasing concentrations of Bbp_{N2N3} (40 nM-2.56 μM) to Fg immobilized on a sensor chip was analyzed using a BIAcore 3000 (Fig.

3A). The results from kinetic and equilibrium analyses revealed $K_{D,S}$ of 510 +/- 5 nM and 540 +/- 7 nM, respectively for the binding of Bbp_{N2N3} to Fg (Fig. 3B). The kinetic studies indicate rapid on and off rates ($5.85 \times 10^4 \text{ M}^{-1} \text{ s}^{-1}$ +/- 0.36 and $2.98 \times 10^2 \text{ s}^{-1}$ +/- 0.16, respectively) and the equilibrium experiment revealed a binding ratio of 1:1 per dimer of Fg. Together, these data demonstrate that Bbp_{N2N3} binds specifically to human Fg with an affinity similar to that of other Fg binding MSCRAMMs (3), (11), (14).

Bbp_{N2N3} recognizes the A α chain of fibrinogen - To locate the Bbp binding site(s) in Fg we used Far Western blotting analysis. Fg was reduced in sample buffer containing dithiothreitol to dissociate disulfide bonds, and the three Fg polypeptides were separated by SDS-PAGE (Fig. 4A) and transferred to a nitrocellulose membrane. The membrane was probed with different recombinant His-tagged MSCRAMMs and binding was revealed with an anti-His antibody. In this assay, Bbp_{N2N3} bound to the A α chain of Fg (Fig. 4B), while SdrG_{N2N3} and ClfA_{N2N3} bound to their previously reported ligands, the B β and γ chains, respectively (4), (14).

In order to verify our Far Western results, binding of Bbp_{N2N3} to the individual Fg chains was tested. Recombinant full-length A α , B β , and γ chains were expressed as His-tagged constructs and purified (Fig. 4C) under denaturing conditions in 8M urea. Individual chains were coated on microtiter plates and the binding of increasing concentrations of Bbp_{N2N3} (15.6-500 nM) to the immobilized Fg polypeptides was followed (Fig. 4D). Whereas Bbp_{N2N3} did not recognize the B β and γ Fg polypeptides, it bound in a concentration-dependent and saturable manner to plasma Fg and recombinant Fg A α indicating that Bbp_{N2N3} binds to a linear sequence in the human Fg A α chain.

The binding site for Bbp lies within residues 561-575 of the Fg A α chain - To map the Bbp_{N2N3} binding site further, we constructed a series of C-terminal truncates of the A α chain (Fig. 5A). The recombinant Fg A α 1-575 and Fg A α 1-560 were purified (Figure 5B lanes 3 and 4, respectively) and examined for their ability to support Bbp binding. Far Western blots revealed that A α 1-575 retained the Bbp_{N2N3} binding site (Fig. 5C, lane 3). However, no MSCRAMM binding was detected to A α 1-560 (Fig. 5C, lane

4), suggesting that Bbp binding to Fg requires a residue(s) in A α 560-575. To confirm our results, a solid phase assay comparing the binding of Bbp_{N2N3} to A α 1-560 and A α 1-575 revealed that only A α 1-575 supported a concentration-dependent binding (Fig. 6A). These results indicate that residues involved in the binding of Bbp_{N2N3} to Fg lie in the A α chain between position 561 and 575.

Full-length Bbp binds to Fg A α chain residues 561-575 - The non-pathogenic bacterium *Lactococcus lactis* has been successfully used as a heterologous host to display full-length forms of MSCRAMMs on its cell surface (23). This system was used to determine whether Bbp expressed on the surface of a bacterium could recognize the binding domain identified for recombinant Bbp_{N2N3} in Fg A α . Using a bacterial adherence assay, we determined that *L. lactis* (pKS80-Bbp) adhered to plates coated with A α 1-575 but not to plates coated with A α 1-560; whereas *L. lactis* carrying the empty pKS80 did not attach to plates coated with either of the A α truncation mutants (Fig. 6B). This result indicates that full-length Bbp expressed on the surface of a bacterium can bind to the identified binding sequence in Fg.

An *S. aureus* Newman mutant that is defective in the MSCRAMMs ClfA, ClfB, IsdA, IsdB, SdrC, SdrD, and SdrE has been constructed (23). This strain was used to express the full-length *bbp* gene under the control of its native promoter. The mutant host carrying the empty vector pCU1 and pCU1-Bbp were tested for adherence to A α 1-575. Newman expressing Bbp attached to wells coated with A α 1-575 but not to immobilized A α 1-560. In contrast, the empty vector control strain did not recognize either A α construct (Fig. 6C). These data indicate that Bbp expressed on the surface of *S. aureus* recognizes the identified binding site and can mediate adherence to human Fg.

Characterization of the interaction between Bbp and Fg A α using synthetic peptides - To further define the binding site in Fg A α for Bbp_{N2N3} we used synthetic peptides in inhibition experiments. Increasing concentrations (0.1-30 μM) of peptides corresponding to different segments of Fg A α were preincubated with Bbp_{N2N3} before the mixture was added to Fg-coated wells (Fig. 7A). The A α 561-575 peptide

fully inhibited the binding of Bbp_{N2N3} to immobilized Fg, whereas a peptide containing the same residues but in a scrambled sequence (A α Scr) did not exhibit any inhibitory activity. In a second assay (Fig. 7B) 100% inhibition was observed with the peptides A α 551-575, A α 561-575 and A α 556-570. However, the A α 551-565 peptide did not affect the binding of Bbp_{N2N3} to Fg.

The interaction between Bbp_{N2N3} and Fg A α peptides was further characterized by isothermal titration calorimetry (ITC). Each peptide was tested for binding by titrating a solution of 225 μ M peptide into a cell containing 15 μ M Bbp_{N2N3} (Fig. 7C, top panels). The one binding site fit model was used to analyze the data, which are summarized in Table 4. ITC analysis showed that the peptides A α 551-575 and A α 561-575 bound to Bbp_{N2N3} with K_{DS}, of 796 nM and 309 nM, respectively, indicating high affinity interactions. Furthermore, no binding to the peptide A α 551-565, was detected suggesting that these residues are not important for binding. These results are consistent with our data using the truncated Fg A α chain mutants. The peptide A α 556-570 bound the MSCRAMM with a K_D of 1.8 μ M. Therefore, residues contained in this peptide can mediate binding to Bbp_{N2N3} albeit with a lower affinity. The affinities of the peptides for Bbp_{N2N3} correlate nicely with the peptide inhibition data (Fig. 7A, B) so that the inhibitory activity exhibited by the peptides directly relates to their ability to bind to Bbp_{N2N3}. Taken together, the truncation analysis experiments, the inhibition data, and the ITC results indicate that Bbp_{N2N3} binds specifically to A α residues 561-575.

A Clustal alignment of the Fg A α 561-575 of Fg from six species was performed (Fig. 7D). The results indicate that the sequences of human, canine and feline fibrinogen are related. All three contain a potential integrin binding RGD site; whereas only some of the identified binding residues are present in porcine or bovine Fg. Furthermore, the rat and murine sequences are more distant from the human sequence in this region. Fg from these rodents does not contain the RGD site, nor a stretch of polar, uncharged residues. The alignment data indicate that the feline and canine Fg are the closest to human, with only minor sequence differences, yet neither Fg is recognized by Bbp_{N2N3} (Fig. 2C). To further

confirm the results obtained with full-length Fg, an inhibition assay was performed with the synthetic peptide corresponding to the A α 561-575 residues in canine Fg. The A α canine peptide did not inhibit the ability of Bbp_{N2N3} to bind to Fg (Fig. 7E). This result verifies our previous data and confirms that Bbp targets a human specific sequence in Fg A α .

Bbp_{N2N3} inhibits fibrin formation – Many MSCRAMMs not only bind to the target molecule in the host but also manipulate the biology of the target. For example SdrG from *S. epidermidis* inhibits coagulation by binding to and covering the thrombin cleavage site in the Fg B β -chain. To examine the effect of Bbp on coagulation, Fg was pretreated with increasing concentrations (0.3-10 μ M) of Bbp_{N2N3}, SdrG_{N2N3}, as a positive control, or BSA as a negative control prior to addition of thrombin. Bbp_{N2N3} inhibited coagulation in a concentration-dependent manner as effectively as SdrG_{N2N3} (Fig. 8A). Human thrombin is capable of cleaving the Fg of other species. Therefore, we examined whether the effect on coagulation exerted by Bbp was species specific. Bbp_{N2N3} did not inhibit thrombin-catalyzed coagulation of ovine Fg (Fig. 8B), which is not recognized by the MSCRAMM. Thus, our results suggest that Bbp can inhibit blood coagulation by binding to Fg.

DISCUSSION

S. aureus appears to use a multitude of virulence factors to cause a wide range of diseases. These virulence factors likely interact with specific molecular targets in the host. Here, we report that Bbp recognizes a specific sequence in the A α polypeptide of human Fg.

We observed that Bbp_{N2N3} can bind to soluble as well as immobilized native Fg, reduced Fg, and recombinant, denatured Fg A α chain. These data indicate that the MSCRAMM binds to a linear sequence in the ligand, which is typical of Fg-binding MSCRAMMs. Furthermore, BIAcore experiments with immobilized Fg revealed a K_D of 540 nM for the Bbp_{N2N3} interaction, and a K_D of 309 nM was calculated from ITC experiments where the peptide A α 561-575 was titrated into a solution of Bbp_{N2N3}. The two methods yielded similar K_D values although, in one case intact immobilized Fg was the binding partner and in the

other a soluble linear Fg peptide was used. This suggests that the peptide sequence contains all Bbp interacting residues in Fg. Furthermore, the K_D determined for the Bbp/Fg peptide interaction is similar to those determined for the binding of Fg peptides to the staphylococcal MSCRAMMs SdrG (380 nM), ClfA (5.8 μ M), and FnbpA (2.4 μ M) even though Bbp binds to a site distinctly different from those recognized by the other Fg-binding MSCRAMMs (3), (11), (27).

Bbp_{N2N3} only targets human Fg demonstrating a high degree of specificity of the interaction. Alignment of the sequences corresponding to the human Fg A α 561-575 in Fg from other species revealed small differences among the residues present in human, feline, and canine Fg. Specifically, the canine sequence contains an extra hydrophobic residue at (human) position 565. This offsets the stretch of polar, uncharged residues found between 565 and 571 by one position. Also, Ser⁵⁶⁹ in human is a Thr in the canine sequence. These are the only two differences between the human and canine sequences, but apparently they are sufficient to abrogate Bbp_{N2N3} binding to canine Fg, as the A α canine peptide had no effect on Bbp_{N2N3} binding to Fg. The structural basis for this remarkable restricted ligand specificity is currently under investigation.

The ability of Bbp to bind Fg was initially demonstrated with recombinant Bbp_{N2N3} and was confirmed using constructs that express the full-length protein on the surface of two bacterial hosts. *L. lactis* and an *S. aureus* Newman mutant devoid of all known fibrinogen binding MSCRAMMs provided a platform to study the ability of the single MSCRAMM to engage in ligand binding (23). In this study, Bbp on the surface of both bacteria mediated attachment to immobilized A α 1-575 but not to A α 1-560 (Figure 3-11b, c). These data indicate that the full-length Bbp protein expressed on the surface of a

bacterium can mediate attachment to a Fg substrate.

The binding site for Bbp_{N2N3} was mapped to A α 561-575 in the Fg molecule, which ends with the second RGDS site of the A α chain. Reports have suggested a role for the second A α RGD site in binding to the integrins $\alpha_5\beta_1$ and $\alpha_v\beta_3$ (28). Although further studies are required in order to determine what downstream effects Bbp binding could have on Fg biology, one possible effect could be a modulation of the Fg A α -integrin interaction.

Experiments demonstrate that Bbp can inhibit thrombin induced blood coagulation. The effect is of a similar potency as that previously observed for SdrG. However, where as SdrG binding to Fg interferes with thrombin-induced release of the fibrinopeptide B, the mechanism of Bbp's anticoagulant action is presently unclear.

Bone sialoprotein was previously described as a ligand of Bbp. This interaction may play a specific role in the pathogenesis of osteomyelitis, an infection of the bone, which may be caused by hematogenous spread. Therefore, it is possible that Bbp may function in two capacities (i) as an important factor in the colonization of bone tissue and (ii) as a contributing factor in *S. aureus* hematologic diseases, such as sepsis. Future studies regarding the expression profile of Bbp in different disease settings or the role of the MSCRAMM in disease-specific models may aid in elucidating the contribution of Bbp to *S. aureus* pathogenesis.

Acknowledgements- The authors wish to acknowledge NARSA for providing *S. aureus* MRSA 252. Drs. Ed Feil, University of Bath, and Ross Fitzgerald, University of Edinburgh, are acknowledged for helpful discussion. T. J. Foster was supported by Science Foundation Ireland and M. Hook was supported by grant AI 20624 from the NIH.

REFERENCES

1. Lowy, F. D. (1998) Staphylococcus aureus infections, *N Engl J Med* 339, 520-532.
2. Foster, T. J., and Höök, M. (1998) Surface protein adhesins of Staphylococcus aureus, *Trends Microbiol* 6, 484-488.

3. Ponnuraj, K., Bowden, M. G., Davis, S., Gurusiddappa, S., Moore, D., Choe, D., Xu, Y., Hook, M., and Narayana, S. V. L. (2003) A "dock, lock, and latch" structural model for a staphylococcal adhesin binding to fibrinogen., *Cell* 115, 217-228.
4. Davis, S. L., Gurusiddappa, S., Mccrea, K. W., and Perkins, S. (2001) SdrG , a Fibrinogen-binding Bacterial Adhesin of the Microbial Surface Components Recognizing Adhesive Matrix Molecules Subfamily from Staphylococcus epidermidis , Targets the Thrombin Cleavage Site in the Bbeta Chain, *Journal of Biological Chemistry* 276, 27799 -27805.
5. Bowden, M. G., Heuck, A. P., Ponnuraj, K., Kolosova, E., Choe, D., Gurusiddappa, S., Narayana, S. V., Johnson, A. E., and Hook, M. (2008) Evidence for the "dock, lock, and latch" ligand binding mechanism of the staphylococcal microbial surface component recognizing adhesive matrix molecules (MSCRAMM) SdrG, *J Biol Chem* 283, 638-647.
6. Kollman, J. M., Pandi, L., Sawaya, M. R., Riley, M., and Doolittle, R. F. (2009) Crystal structure of human fibrinogen, *Biochemistry* 48, 3877-3886.
7. Mosesson, M. W., Siebenlist, K. R., and Meh, D. A. (2001) The structure and biological features of fibrinogen and fibrin, *Ann N Y Acad Sci* 936, 11-30.
8. Gailit, J., Clarke, C., Newman, D., Tonnesen, M. G., Mosesson, M. W., and Clark, R. A. (1997) Human fibroblasts bind directly to fibrinogen at RGD sites through integrin alpha(v)beta3, *Exp Cell Res* 232, 118-126.
9. McDevitt, D., Francois, P., Vaudaux, P., and Foster, T. J. (1994) Molecular characterization of the clumping factor (fibrinogen receptor) of Staphylococcus aureus, *Mol Microbiol* 11, 237-248.
10. Ni Eidhin, D., Perkins, S., Francois, P., Vaudaux, P., Hook, M., and Foster, T. J. (1998) Clumping factor B (ClfB), a new surface-located fibrinogen-binding adhesin of Staphylococcus aureus, *Mol Microbiol* 30, 245-257.
11. Wann, E. R., Gurusiddappa, S., and Hook, M. (2000) The fibronectin-binding MSCRAMM FnbpA of Staphylococcus aureus is a bifunctional protein that also binds to fibrinogen, *J Biol Chem* 275, 13863-13871.
12. Rivera, J., Vannakambadi, G., Hook, M., and Speziale, P. (2007) Fibrinogen-binding proteins of Gram-positive bacteria, *Thromb Haemost* 98, 503-511.
13. Walsh, E. J., Miajlovic, H., Gorkun, O. V., and Foster, T. J. (2008) Identification of the Staphylococcus aureus MSCRAMM clumping factor B (ClfB) binding site in the aC-domain of human fibrinogen, *Microbiology*, 550-558.
14. McDevitt, D., Nanavaty, T., House-Pompeo, K., Bell, E., Turner, N., McIntire, L., Foster, T., and Hook, M. (1997) Characterization of the interaction between the Staphylococcus aureus clumping factor (ClfA) and fibrinogen, *Eur J Biochem* 247, 416-424.
15. Hair, P. S., Ward, M. D., Semmes, O. J., Foster, T. J., and Cunnion, K. M. (2008) Staphylococcus aureus clumping factor A binds to complement regulator factor I and increases factor I cleavage of C3b, *J Infect Dis* 198, 125-133.
16. Walsh, E. J., O'Brien, L. M., Liang, X., Hook, M., and Foster, T. J. (2004) Clumping factor B, a fibrinogen-binding MSCRAMM (microbial surface components recognizing adhesive matrix molecules) adhesin of Staphylococcus aureus, also binds to the tail region of type I cytokeratin 10, *J Biol Chem* 279, 50691-50699.
17. Holden, M. T., Feil, E. J., Lindsay, J. A., Peacock, S. J., Day, N. P., Enright, M. C., Foster, T. J., Moore, C. E., Hurst, L., Atkin, R., Barron, A., Bason, N., Bentley, S. D., Chillingworth, C., Chillingworth, T., Churcher, C., Clark, L., Corton, C., Cronin, A., Doggett, J., Dowd, L., Feltwell, T., Hance, Z., Harris, B., Hauser, H., Holroyd, S., Jagels, K., James, K. D., Lennard, N., Line, A., Mayes, R., Moule, S., Mungall, K., Ormond, D., Quail, M. A., Rabinowitsch, E., Rutherford, K., Sanders, M., Sharp, S., Simmonds, M., Stevens, K., Whitehead, S., Barrell, B. G., Spratt, B. G., and Parkhill, J. (2004) Complete genomes of two clinical Staphylococcus aureus strains: evidence for the rapid evolution of virulence and drug resistance, *Proc Natl Acad Sci U S A* 101, 9786-9791.

18. Lord, S. T. (1985) Expression of a cloned human fibrinogen cDNA in *Escherichia coli*: synthesis of an A alpha polypeptide, *DNA* 4, 33-38.
19. Bolyard, M., and Lord, S. (1989) Expression in *Escherichia coli* of the human fibrinogen B beta chain and its cleavage by thrombin, *Journal of Biological Chemistry*, 1202-1206.
20. Bolyard, M. G., and Lord, S. T. (1988) High-level expression of a functional human fibrinogen gamma chain in *Escherichia coli*., *Gene* 66, 183-192.
21. Carson, M. (1997) Ribbons, *Methods Enzymol* 277, 493-505.
22. Hartford, O., O'Brien, L., Schofield, K., Wells, J., and Foster, T. J. (2001) The Fbe (SdrG) protein of *Staphylococcus epidermidis* HB promotes bacterial adherence to fibrinogen, *Microbiology* 147, 2545-2552.
23. Corrigan, R. M., Miajlovik, H., and Foster, T. J. (2009) Surface proteins that promote adherence of *Staphylococcus aureus* to human desquamated nasal epithelial cells., *BMC Microbiology* 9.
24. Larkin, M. A., Blackshields, G., Brown, N. P., Chenna, R., McGettigan, P. A., McWilliam, H., Valentin, F., Wallace, I. M., Wilm, A., Lopez, R., Thompson, J. D., Gibson, T. J., and Higgins, D. G. (2007) Clustal W and Clustal X version 2.0, *Bioinformatics* 23, 2947-2948.
25. Josefsson, E., McCrea, K. W., Ni Eidhin, D., O'Connell, D., Cox, J., Hook, M., and Foster, T. J. (1998) Three new members of the serine-aspartate repeat protein multigene family of *Staphylococcus aureus*, *Microbiology* 144 (Pt 12), 3387-3395.
26. Deivanayagam, C. C., Perkins, S., Danthuluri, S., Owens, R. T., Bice, T., Nanavathy, T., Foster, T. J., Hook, M., and Narayana, S. V. (1999) Crystallization of ClfA and ClfB fragments: the fibrinogen-binding surface proteins of *Staphylococcus aureus*, *Acta Crystallogr D Biol Crystallogr* 55, 554-556.
27. Ganesh, V. K., Rivera, J. J., Smeds, E., Ko, Y.-P., Bowden, M. G., Wann, E. R., Gurusiddappa, S., Fitzgerald, J. R., and Höök, M. (2008) A structural model of the *Staphylococcus aureus* ClfA-fibrinogen interaction opens new avenues for the design of anti-staphylococcal therapeutics., *PLoS pathogens* 4, 1-10.
28. Suehiro, K., Mizuguchi, J., Nishiyama, K., Iwanaga, S., Farrell, D. H., and Ohtaki, S. (2000) Fibrinogen binds to integrin alpha(5)beta(1) via the carboxyl-terminal RGD site of the Aalpha-chain, *J Biochem* 128, 705-710.

FIGURE LEGENDS

Figure 1. Bbp_{N2N3} construct. (A) Domain organization of full length Bbp (top) and Bbp_{N2N3} (bottom) showing the (S) signal sequence, (N1, N2, N3) amino terminal subdomains of A region, (B1, B2, B3) B-repeats, (SD) Serine-Aspartate repeat region, (W) wall domain, (M) membrane domain, (C) carboxy-terminus. In Bbp_{N2N3}, (H) Hexahistidine tag. (B) Ribbon representation of the homology model of the N2N3 subdomains of Bbp. The N2 and the N3 subdomains are colored respectively in green and yellow. (C) Purified Bbp_{N2N3} (1 µg/lane) was analyzed by SDS-PAGE Coomassie blue staining (lane 1) or transferred to nitrocellulose for anti-His (lane 2) followed by goat-anti-mouse-AP blotting.

Figure 2. Bbp_{N2N3} binds to fibrinogen. (A) A ligand screen was performed on immobilized extracellular matrix and plasma proteins. The putative ligands were immobilized on microtiter wells and probed with increasing concentrations (0.1-10 µM) of Bbp_{N2N3} followed by rabbit-anti-Bbp_{N2N3} and goat-anti-rabbit-HRP. (B) Increasing amounts of Bbp_{N2N3} (0.25 to 2.5 µg) were coated on microtiter wells and probed with 1 µM Fg followed by goat-anti-human Fg and donkey-anti-goat-HRP. (C) Microtiter wells were coated with 1 µg of human, canine, feline, bovine, ovine, murine, or porcine Fg, or BSA in bicarbonate buffer overnight. The wells were probed with 500 nM Bbp_{N2N3} or ClfA_{N2N3}, followed by protein specific rabbit polyclonal antibodies and goat-anti-rabbit-HRP. Values represent the mean +/- the standard error of the mean.

Figure 3. Surface Plasmon Resonance (SPR) analysis of Bbp_{N2N3} binding to fibrinogen. Two-fold linear dilution series (2.56 to 0.04 μ M) of Bbp_{N2N3} were injected over the Fg surface (1600 RU) on a Biacore sensor chip. (A) Kinetics analysis. Baseline corrected response curves for each injection of Bbp_{N2N3} (shown as black lines with lower concentration at the bottom) are overlaid with the global fitting to a 1:1 (Langmuir) binding model (shown in red). Kinetic rate constants as well as response maximum (R_{max}) listed in the inset were obtained from the fitting. (B) Equilibrium analysis: Responses at equilibrium of the SPR curves were fit to a one-site binding (hyperbola) isotherm (GraphPad Prism 4) to obtain the dissociation equilibrium constant and binding maximum (B_{max}). Data consist of one representative of three experiments. Values represent the mean +/- the standard error of the mean.

Figure 4. Bbp_{N2N3} recognizes the A α chain of fibrinogen. Fg was reduced and separated on SDS-PAGE followed by Coomassie staining (A) to reveal the three chains A α (top band), B β (middle band) and γ (bottom band) or electrotransferred for Far Western blotting (B). Membranes were probed with Bbp_{N2N3} (left), SdrG_{N2N3} (middle), and ClfA_{N2N3} (right) followed by incubation with protein-specific rabbit polyclonals and goat-anti-rabbit-AP. (C) Recombinant His-tagged constructs of the individual chains were purified, run on SDS-PAGE and stained with Coomassie for comparison to reduced human Fg. (D) Fg and recombinant individual A α , B β , and γ chains were coated on microtiter wells and probed with Bbp_{N2N3} followed by anti-Bbp_{N2N3} and goat-anti-rabbit-HRP. Values represent the mean +/- the standard error of the mean.

Figure 5. The Bbp_{N2N3} binding site on A α lies in residues 561-575. (A) Schematic of full-length A α (1-625) and C'-truncated (A α 1-575 and A α 1-560) constructs. (B) Reduced plasma Fg (lane 1), purified A α (lane 2), A α 1-575 (lane 3), A α 1-560 (lane 4), B β (lane 5), and γ (lane 6) chains were separated on SDS-PAGE. (C) Far western on Fg constructs was performed by incubating the membrane with Bbp_{N2N3}, followed by rabbit-anti-Bbp_{N2N3} and goat-anti-rabbit AP.

Figure 6. Recombinant Bbp_{N2N3} and full-length Bbp on the surface of cells bind to Fg A α 1-575. Wells coated with purified A α 1-575 or A α 1-560 were probed with Bbp_{N2N3} (A) followed by rabbit-anti-Bbp_{N2N3} polyclonal antibody then with goat-anti-rabbit-HRP to detect binding. (B and C) Adherence of bacteria to A α 1-575 or A α 1-560 was detected with crystal violet staining. Microtiter wells with coated A α 1-575 or A α 1-560 were incubated with *L. lactis*-pKS80 and *L. lactis*-pKS80-Bbp (B) or with *S. aureus* Newman DU6023-pCU1 and *S. aureus* Newman DU6023-pCU1-Bbp (C). Values represent the mean +/- the standard error of the mean.

Figure 7. Analysis of the interaction between Bbp_{N2N3} and Fg A α peptides. Increasing concentrations of the peptides A α 561-575 and A α Scr (A); A α 551-575, A α 561-575, A α 556-570, and A α 551-565 (B); or A α 561-575 and A α Canine (E) were preincubated with Bbp_{N2N3} (150 nM) for 30 minutes before addition to Fg coated wells in a solid-phase assay to assess inhibition of binding. Values represent the mean +/- the standard error of the mean. (C) Isothermal titration calorimetry of 225 μ M Fg A α peptides and 15 μ M Bbp_{N2N3} was measured with a VP-ITC. Thirty titrations of 10 μ l peptides were injected into the cell containing Bbp_{N2N3} (top panels). The data were fitted to one-binding site model (bottom panels), and binding affinities are expressed as dissociation constants (K_D) or the reciprocal of the association constants determined by Origin software; (N.D., affinity not determined). (D) Clustal alignment of the residues corresponding to the human sequence A α 561-575 from different species. Coloring based on physico-chemical properties of the amino acids. Red: small, hydrophobic, and aromatic; blue: acidic; magenta: basic; green: hydroxyl and amine plus basic.

Figure 8. Bbp_{N2N3} inhibits fibrin formation. Increasing concentrations (0.3– 10 μ M) (A) or 1 μ M (B) of BSA, SdrG_{N2N3}, or Bbp_{N2N3} were preincubated with human Fg-coated (A and B) or ovine Fg-coated (B) wells prior to the addition of α -thrombin. Values represent the mean +/- the standard error of the mean.

Table 1. Oligonucleotides used in this study.

Primer name	Oligonucleotide sequence
pQE30-BbpF	<u>CCCGGATCCGTTGCTTCAAACAATGTTAATGAT</u>
pQE30-BbpR	<u>CCCAAGCTTTTATTTCAGGTTAACAGTACCGTCACC</u>
pQE30-FgA α 1F	<u>CGGGATCCGCAGATAGTGGTGAAGGT</u>
pQE30-FgA α 1-575R	<u>CGAAGCTTTT</u> AGGAGTCTCCTCTGTTGTAAC
pQE30-FgA α 1-560R	<u>CGAAGCTTTT</u> AGTAAGTGAAGATTACCACG
pCU1-BbpPrF	<u>CGGGATCCGATATAACATACATCAACAT</u>
pCU1-BbpTrR	<u>CGTCTAGAATATTATCGCCTCATATAAG</u>

Restriction sites are underlined.

Table 2. Constructs used in this study.

Construct	Vector	Residues	Source
<i>E. coli</i> Bbp _{N2N3}	pQE30	270-599	This study
<i>E. coli</i> SdrG _{N2N3}	pQE30	273-597	(3)
<i>E. coli</i> ClfA _{N2N3}	pQE30	229-545	(27)
<i>E. coli</i> Fg A α	pQE30	Full length mature A α	(18)
<i>E. coli</i> Fg A α 1-575	pQE30	1-575 of mature A α	This study
<i>E. coli</i> Fg A α 1-560	pQE30	1-560 of mature A α	This study
<i>E. coli</i> Fg B β	pQE30	Full length mature B β	(19)
<i>E. coli</i> Fg γ	pQE30	Full length mature γ	(20)
<i>L. lactis</i> -vector	pKS80	Empty vector	(23)
<i>L. lactis</i> -Bbp	pKS80	Full length Bbp	This study
<i>S. aureus</i> Newman DU6023-pCU1	pCU1	Empty vector	(23)
<i>S. aureus</i> Newman DU6023-pCU1-Bbp	pCU1	Full length Bbp (with promoter and terminator)	This study

Table 3. Peptides synthesized for this study

Peptide name	Peptide sequence
Fg A α 551-575	FPSRGKSSSYSKQFTSSTSYNRGDS
Fg A α 551-565	FPSRGKSSSYSKQFT
Fg A α 556-570	KSSSYSKQFTSSTSY
Fg A α 561-575	SKQFTSSTSYNRGDS
Fg A α Scr	TSSTRGDSSYNSKQF
Fg A α Canine	SKQFVTSSTTYNRGDS

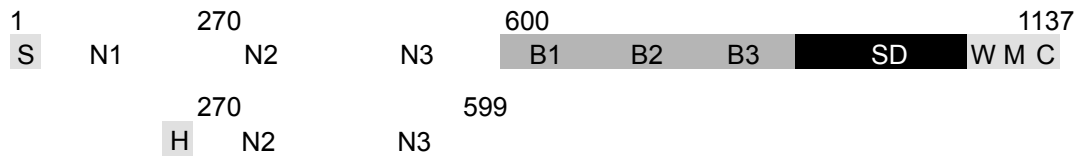
Table 4. Isothermal Titration Calorimetry data

	N	K	ΔH (kcal/mol)	ΔS (kcal/mol)	K_D (calc)
551-575	2.074	1.26E+06	-1.27E+04	-13.95	0.796 μM
551-565	N.D.	N.D.	N.D.	N.D.	N.D.
556-570	1.894	5.48E+05	-1.04E+04	-8.03	1.825 μM
561-575	1.902	3.23E+06	-1.22E+04	-10.51	0.309 μM

N.D. Not determined

Figure 1

A



B



C

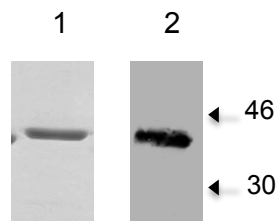


Figure 2

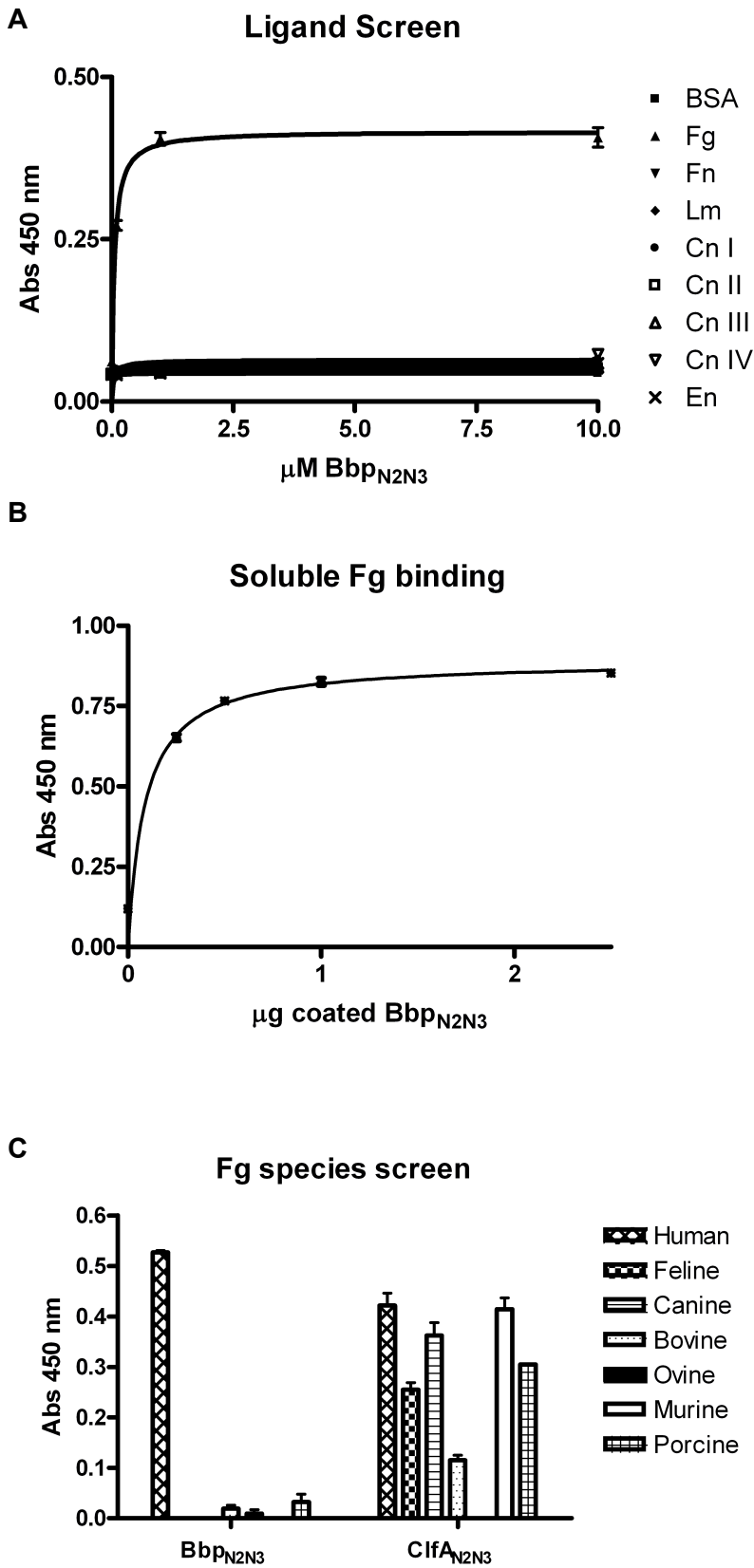


Figure 3

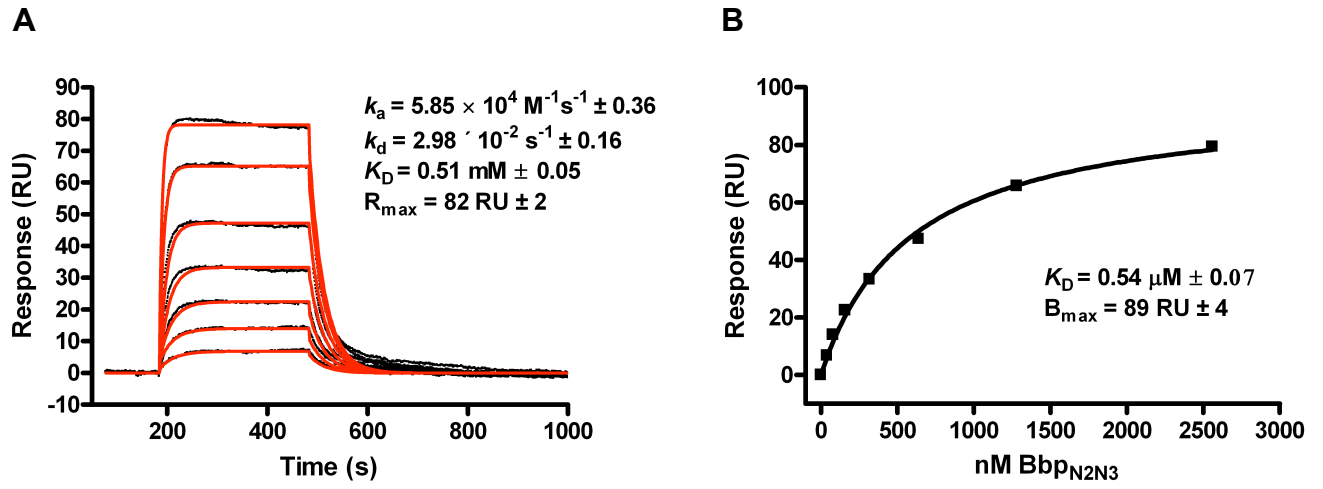


Figure 4

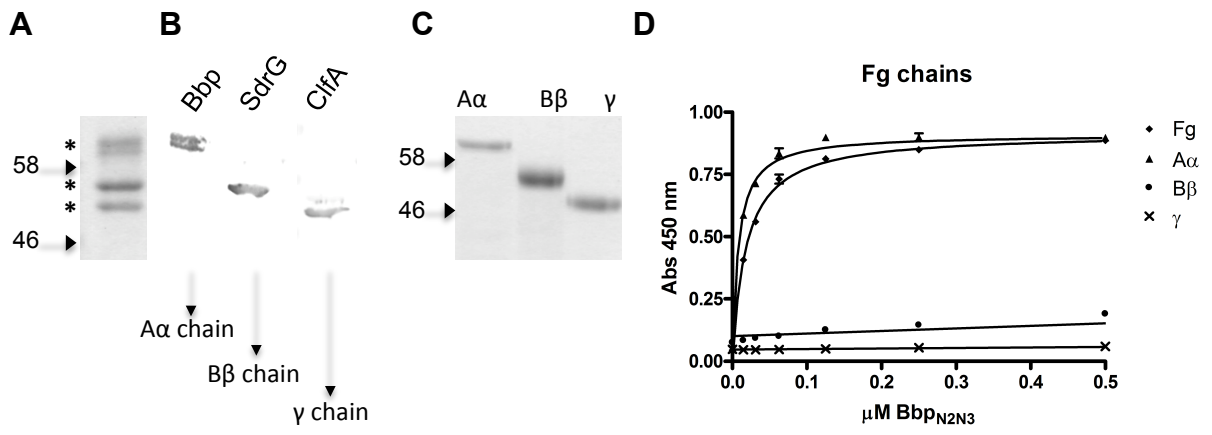


Figure 5

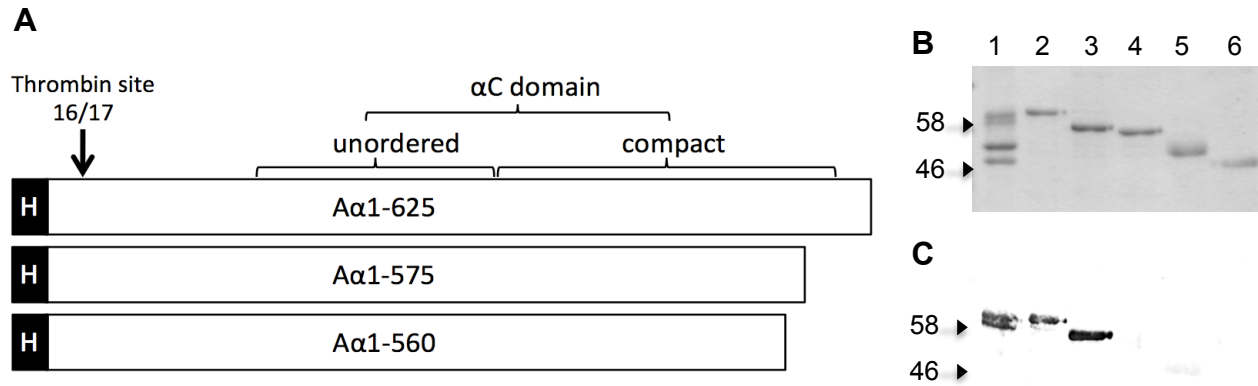


Figure 6

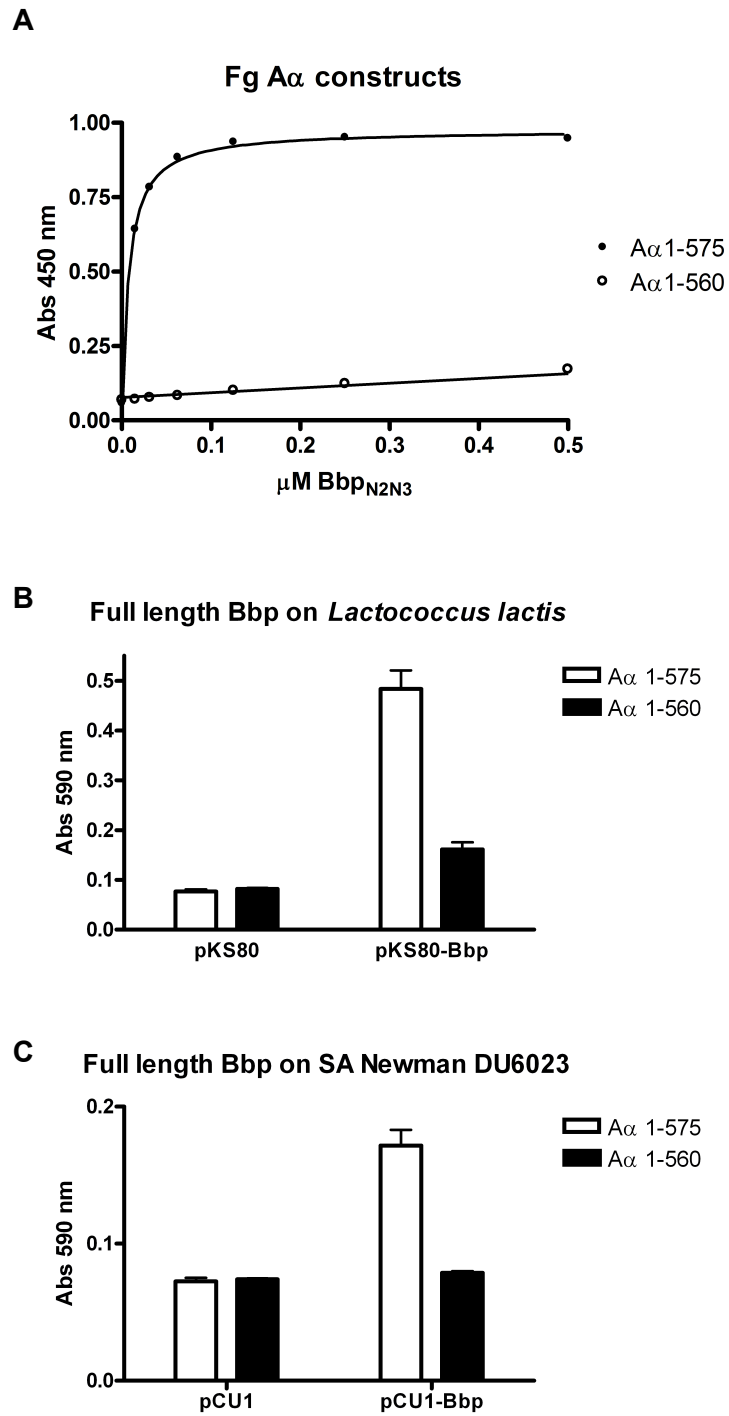


Figure 7

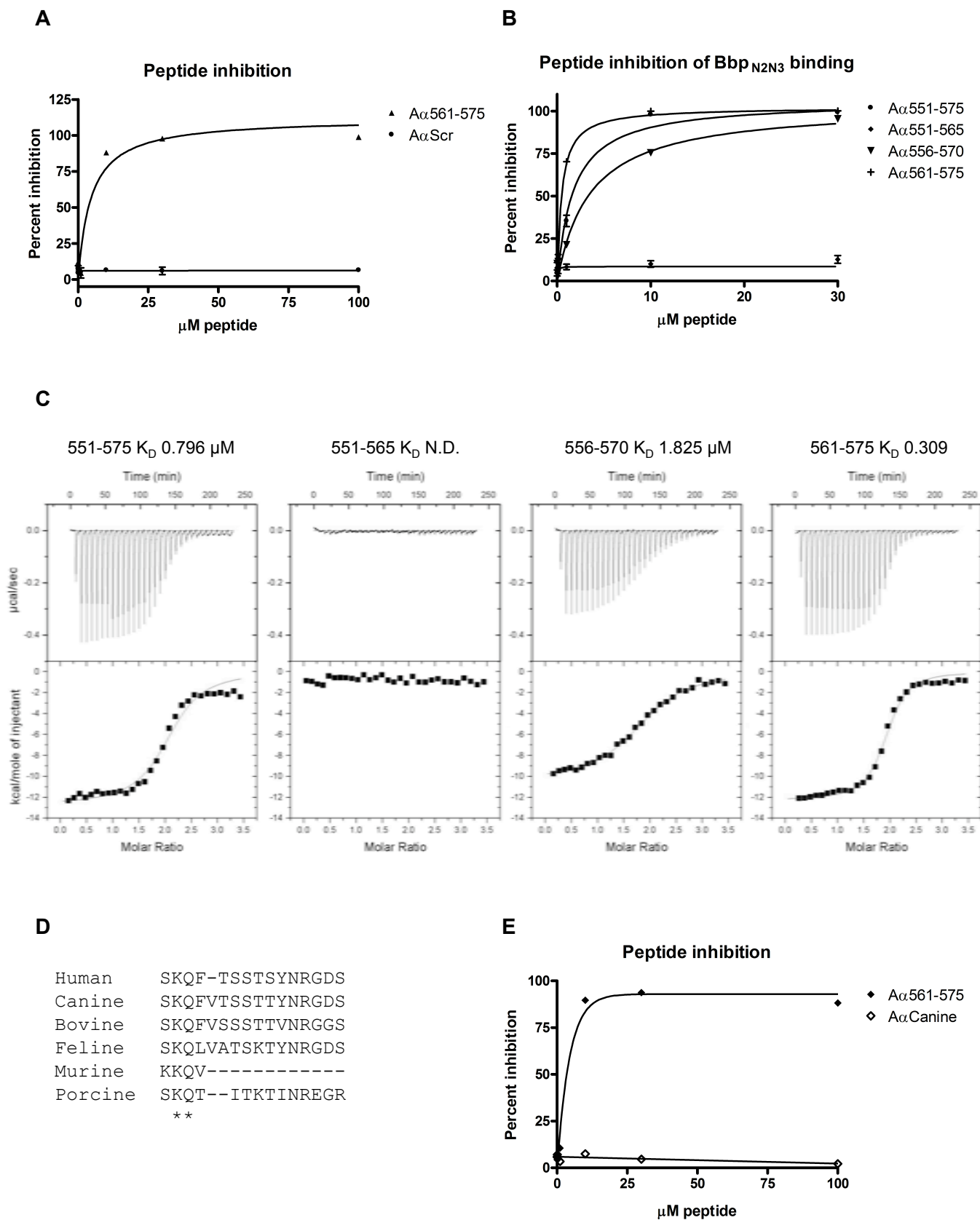


Figure 8

